Research Article

Cancer Prevention Research

Transcriptional Attenuation in Colon Carcinoma Cells in Response to Butyrate

Maria C. Daroqui and Leonard H. Augenlicht

Abstract

The short-chain fatty acid sodium butyrate (NaB), produced in the colonic lumen, induces cell cycle arrest, differentiation, and/or apoptosis in colorectal carcinoma cells *in vitro*, establishing a potential role for NaB in colon cancer prevention. We have previously shown that butyrate decreases *cyclin D1* and *c-myc* expression, each essential for intestinal tumor development, by transcriptional attenuation. Here, we determined that butyrate-induced transcriptional attenuation of the *cyclin D1* and c-*myc* genes in SW837 human colorectal adenocarcinoma cells occurs at ~100 nucleotides downstream of the transcription start site, with a similar positioning in Caco-2 cells. A concomitant decrease in RNA polymerase II occupancy at the 5′ end of each gene was observed. Because transcriptional regulation is associated with chromatin remodeling, we investigated by chromatin immunoprecipitation whether the histone deacetylase inhibitory activity of butyrate altered chromatin structure at the attenuated loci. Although the distributions of histone H3 trimethylated on K4 and K36 along the *cyclin D1* and c-*myc* genes were consistent with current models, butyrate induced only modest decreases in these modifications, with a similar effect on acetylated H3 and a modest increase in histone H3 trimethylated on K27. Finally, transcriptome analysis using novel microarrays showed that butyrate-induced attenuation is widespread throughout the genome, likely independent of transcriptional initiation. We identified 42 loci potentially paused by butyrate and showed that the transcription patterns are gene specific. The biological functions of these loci encompass a number of effects of butyrate on the physiology of intestinal epithelial cells. *Cancer Prev Res; 3(10); 1292–302. ©2010 AACR.*

Introduction

The short-chain fatty acid butyrate is produced in the colon by fermentation of dietary fiber, which generates levels of ~20 mmol/L in the colonic lumen, well above the 2 to 5 mmol/L concentration that induces cell cycle arrest and differentiation in culture (1–3). Colonic epithelial cells *in vivo* use these high levels as their principal energy source (4), and efficient metabolism of short-chain fatty acids is necessary for their induction of colon cell maturation (5, 6). Gene expression profiling showed that, in culture, butyrate altered the steady-state levels of ~7% of the genes interrogated, either increasing or decreasing expression monotonically with time (7). This implied an orderly cascade of events, with successive stages in cell maturation driven by sequential recruitment of genes and pathways, a hallmark of an integrated response necessary for intestinal tissue homeostasis.

c-*myc* and *cyclin D1* are genes downregulated by butyrate during colonic cell maturation. *Cyclin D1* is a driving component of the cell division cycle, and *c-myc* stimulates cell cycling and is important in differentiation as cells migrate from the crypt toward the intestinal lumen (8). Moreover, both genes are direct targets of Wnt signaling (9, 10), a fundamental pathway deregulated in colon tumors, most commonly by mutation of Apc, which alters the transcription mediated by β-catenin-T-cell factor targeting the *cyclin D1*, c-*myc*, and other genes (11). Targeted inactivation of either c-*myc* or *cyclin D1* reduces Apc-initiated intestinal tumor formation, showing that both are essential for tumorigenesis (12, 13). Thus, butyrate-mediated decreased expression of *cyclin D1* and *c-myc* may be fundamental to its chemopreventive activity (14, 15).

Transcriptional attenuation or pausing, first recognized for *c-fos*, *c-myb*, *adenosine deaminase*, *tubulin*, and *cyclooxygenase-2* (16–20), is now understood to be fundamental for the regulation of many inducible as well as constitutively expressed genes (21, 22). In colorectal carcinoma cells, a transcriptional block in response to butyrate was shown by Heruth and coworkers (14) for *c-myc*, which was further explored by us (23). *Cyclin D1*

Authors' Affiliation: Department of Oncology, Albert Einstein Cancer Center, Montefiore Medical Center, Bronx, New York

Note: Supplementary data for this article are available at Cancer Prevention Research Online (http://cancerprevres.aacrjournals.org/).

Corresponding Author: Maria C. Daroqui, Department of Oncology, Montefiore Medical Center, 111 East 210th Street, Bronx, NY 10467. Phone: 718-920-2093; Fax: 718-882-4464; E-mail: cdaroqui@montefiore.org.

doi: 10.1158/1940-6207.CAPR-10-0083

transcriptional downregulation, however, was reported to be associated with transcription factors acting at the promoter in response to histone deacetylase (HDAC) inhibitors and other agents (15, 24). We used imaging of growing transcripts at their site of synthesis to show that *cyclin D1* was also transcriptionally paused by butyrate downstream of the transcription start site (TSS; ref. 25). Thus, transcriptional pausing of *c-myc* and *cyclin D1* by butyrate can play a major role in determining steady-state mRNA levels (23, 25).

Transcriptional regulation is associated with chromatin landmarks, such as specific histone modifications (reviewed in ref. 26). In this regard, butyrate is an inhibitor of HDAC activity, which leads to histone hyperacetylation and chromatin remodeling of induced target genes, whereas histone hypoacetylation has been associated with transcriptionally silent chromatin (27, 28). Here, we first determined the position near the 5′ end at which transcriptional pausing of *c-myc* and *cyclin D1* is initiated by butyrate, as well as chromatin modification along the length of the gene-coding regions. We then extended the investigation to the transcriptome level using novel microarrays, identifying a subset of sequences for which butyrate induced transcriptional pausing. This regulation by butyrate was highly complex and gene specific, and the data suggest that the attenuation mechanism is independent

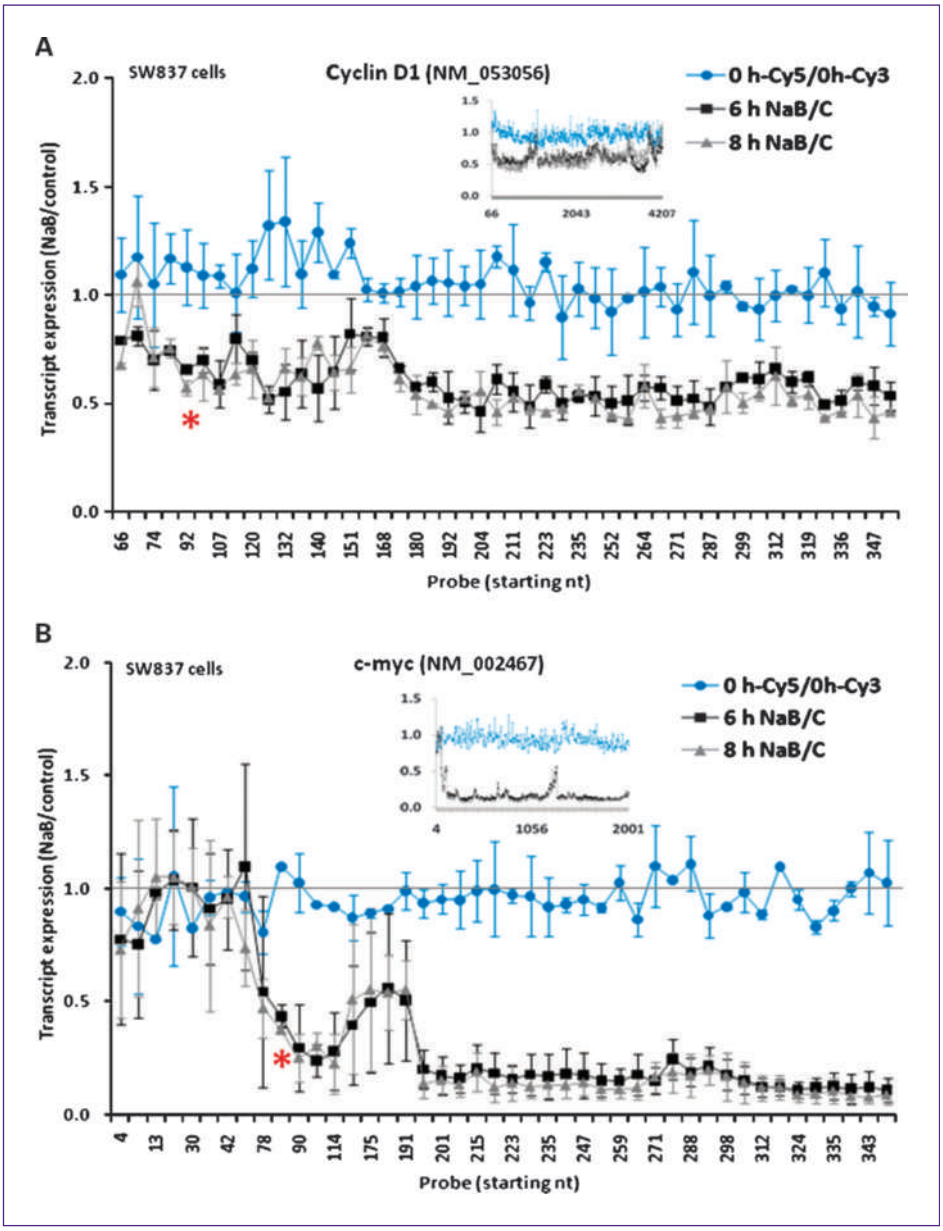

Fig. 1. Cyclin D1 and c-myc transcript expression in response to butyrate. SW837 cells were treated for 0, 6, and 8 h with 5 mmol/L NaB, and cDNA was synthesized and hybridized to a tiling microarray (Materials and Methods). The ratio of NaB-treated (Cy5-labeled) to untreated (Cy3-labeled) cells at each time point of treatment is shown for the first 355 nucleotides of the *cyclin D1* (A) and *c-myc* (B) sequences. Points, mean from three independent experiments; bars, SD. On the abscissa, the probe numbers indicate the first nucleotide of the probe. Insets, ratio of NaB-treated to untreated cells for every probe on the array for each sequence (color-coded as in the main figure). *, position where transcriptional attenuation was induced by NaB. nt, nucleotide.

of mechanisms that determine the frequency of transcriptional initiation.

Materials and Methods

Cells and butyrate treatment

Human colorectal adenocarcinoma SW837 cells (CCL-235) and Caco-2 cells (HTB-37) were grown as described (23, 29) and monitored for *Mycoplasma* contamination (Mycoplasma Plus PCR Primer Set, Agilent Technologies). Exponentially growing cells at ~70% confluency were treated or not with 5 mmol/L (SW837 cells) or 2 mmol/L (Caco-2 cells) sodium butyrate (NaB; Sigma) for different time periods. A lower concentration of NaB was used in Caco-2 cells, as these cells are more sensitive to butyrate induction of cell death.

RNA and probe preparation

RNA was isolated from cells treated or not with NaB for different time periods. Double-stranded cDNA for microarrays was synthesized from RNA as described (NimbleGen) using SuperScript cDNA synthesis kit (Invitrogen). Details are given in Supplementary Methods.

Custom-designed oligonucleotide microarrays

cDNA gene expression arrays were designed and manufactured in collaboration with NimbleGen. Two oligonucleotide arrays were used: "5′ 3′ array" and "tiling array." Details are provided in Supplementary Methods.

Histone purification and Western blot analysis

Western blot analysis and isolation of acid soluble histones were done as described (7, 30). Details are given in Supplementary Methods.

Chromatin immunoprecipitation

To study polymerase II (Pol II) occupancy and histone modification at a specific sequence, chromatin immunoprecipitation assay was done as described in detail in Supplementary Methods.

Quantitative real-time PCR

cDNA from butyrate-treated and untreated cells, as well as DNA isolated by chromatin immunoprecipitation, was analyzed by quantitative real-time PCR using SYBR Green (Applied Biosystems) following the manufacturer's protocol, as described in Supplementary Methods.

Analysis of gene ontology and chromosome distribution

Each sequence potentially paused by butyrate based on the 5′ 3′ array data was classified according to its gene ontology by DAVID Bioinformatics Resources 2008 (NIAID/NIH), as described in Supplementary Methods.

Statistical analysis

The mean value of replicates was analyzed using Student's *t* test. One-way ANOVA and Bonferroni multiple comparison test were used to analyze the data from the tiling array. Results were considered significant when $P < 0.05$.

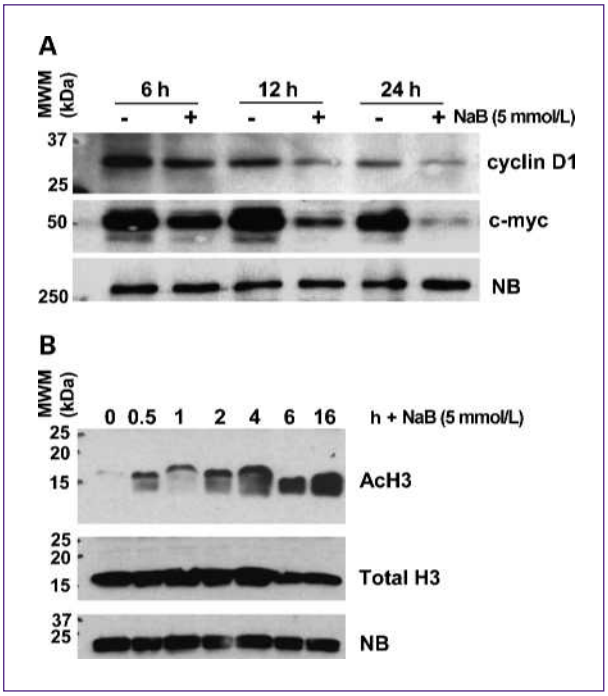

Fig. 2. Effect of butyrate on cyclin D1 and c-myc protein expression and histone modification. A, Western blot for cyclin D1 and c-myc at 6 to 24 h of butyrate treatment. B, AcH3 levels in response to 30 min to 16 h of butyrate treatment. The total level of histone H3 is also shown. NB, nonspecific band.

Results

Transcription of the *cyclin D1* and *c-myc* genes

We first analyzed the effects of NaB on the transcription of *cyclin D1* and *c-myc* in human colorectal adenocarcinoma SW837 cells using a custom-designed oligonucleotide array that tiled through the length of these sequences (Materials and Methods). These arrays were hybridized to Cy3-labeled (untreated, cycling cells) or Cy5-labeled (butyrate-treated cells) cDNA transcribed from total, nuclear, or cytoplasmic RNA. Cells were treated with 5 mmol/L NaB for 0, 6, or 8 hours, time points that preceded the G_1 arrest and apoptosis induced by NaB at ~24 hours (not shown). Figure 1 focuses on the expression level across the first 355 nucleotides of each sequence, shown as the average ratio of three independent experiments, and the insets show the expression throughout the entire coding regions. As expected, the ratio of hybridization of probes from untreated cells labeled with either fluorochrome was approximately 1 along each sequence (Fig. 1). For *cyclin D1*, 6 or 8 hours of butyrate treatment decreased its expression by ~50%, beginning at nucleotide 92 (Fig. 1A). There was a similar pattern for *c-myc*, with its expression decreased by 80% to 90%

downstream of nucleotide 84 (Fig. 1B). The repressed levels of both genes generally persisted throughout the length of each sequence (Fig. 1, insets). A normalization step was done for each of the 628 and 347 probes for *cyclin D1* and *c-myc*, respectively (see Materials and Methods). ANOVA for the NaB-treated data sets (after normalization) versus untreated cells (0 hours), followed by Bonferroni multiple comparison test, showed a highly significant difference at both 6 and 8 hours ($P < 0.0001$), but no significant difference between 0-hour Cy3 and 0-hour Cy5. We further investigated the effects of NaB on *cyclin D1* and *c-myc* transcription in another human colorectal adenocarcinoma cell line, Caco-2, and similar results were obtained. For *cyclin D1*, the decrease in transcript expression was localized at nucleotide 107 (Supplementary Fig. S1A). For *c-myc*, the decrease was somewhat further downstream, at nucleotide 186 (Supplementary Fig. S1B), but still well within the 5′ untranslated region of the message, thus abrogating the generation of a full-length coding mRNA in Caco-2 cells, as it did in SW837 cells. In both cell lines, there were highly reproducible spikes in the generally consistent pattern of repression along both sequences, which could be related to differential hybridization of some probes on the array, despite precautions taken in designing the arrays [e.g., Fig. 1 (insets) and Fig. 5B]. By Western blot, we confirmed that *cyclin D1* and *c-myc* expression was ultimately reduced by NaB at the protein level between 6 and 24 hours of treatment (Fig. 2A).

RNA Pol II occupancy and histone modification along cyclin D1 and c-myc

In untreated SW837 cells, analysis of Pol II by chromatin immunoprecipitation revealed a higher occupancy toward the 5′ end, relative to the rest of the sequence, in the *cyclin D1* gene, whereas more similar levels were observed throughout the length of c-myc (Fig. 3A, black columns). Following butyrate treatment of the cells for 6 hours, Pol II occupancy for cyclin D1 decreased most substantially in exon 1 (nucleotides 1-407), as shown in Fig. 3A (gray columns). Whereas the butyrate-induced difference at the 5′ end of cyclin D1 was not

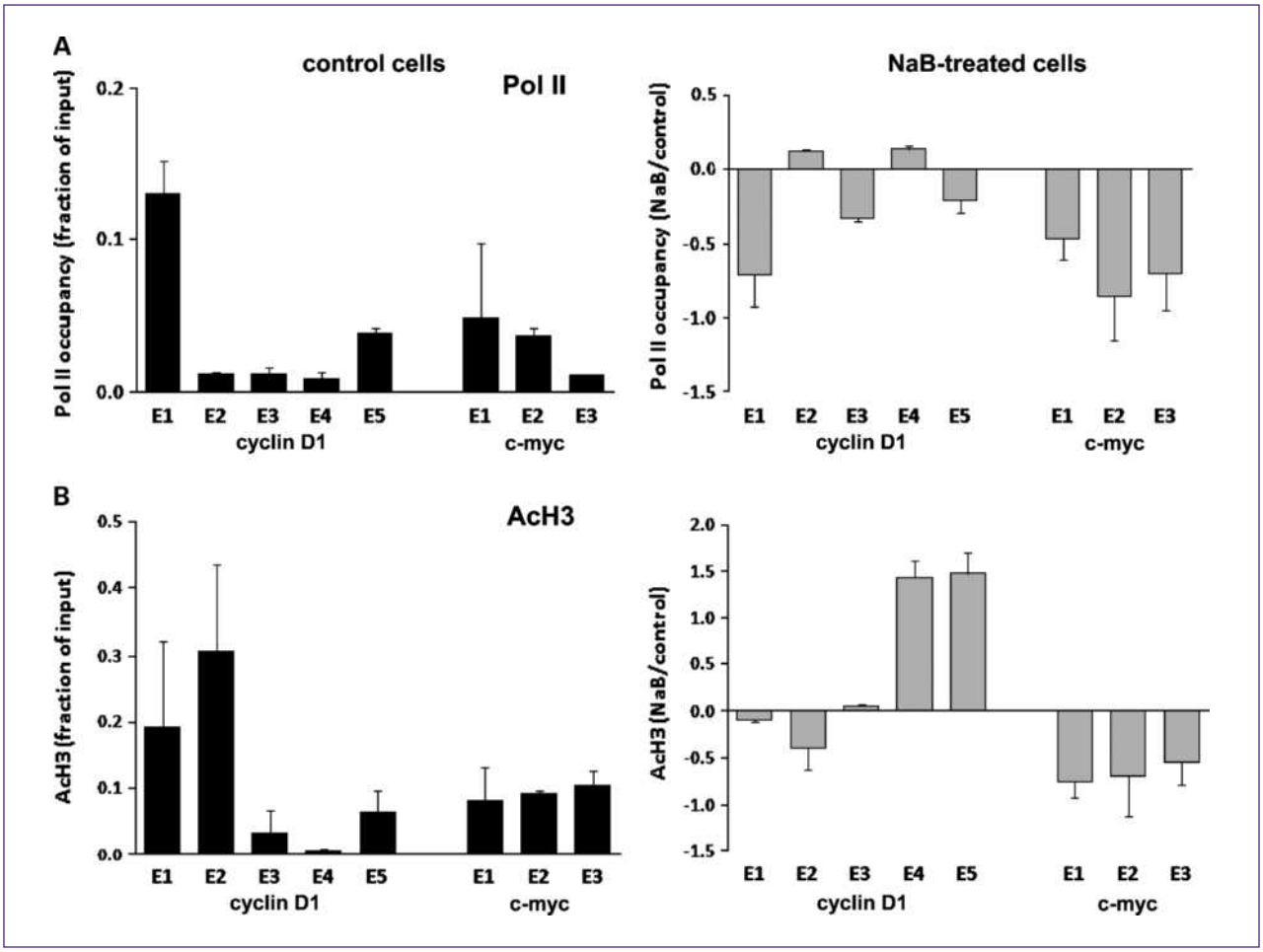

Fig. 3. Chromatin immunoprecipitation of Pol II and modified histones. A, Pol II occupancy at 6 h of butyrate treatment (5 mmol/L) along the five and three exons that make up the *cyclin D1* and *c-myc* coding sequences, respectively. B, AcH3 levels throughout each sequence.

observed downstream, for *c-myc* the pattern was different, with the butyrate-induced decrease being maintained at approximately the same level in exons 2 and 3 (Fig. 3A).

Based on the well-characterized activity of butyrate as a general inhibitor of HDACs (31), we determined the effects of butyrate on chromatin remodeling. An ~8-fold increase in the overall level of histone H3 acetylation (AcH3) at 30 minutes following butyrate treatment was observed and persisted for ~6 hours (Fig. 2B). Despite this overall induction of AcH3, it has been reported that butyrate

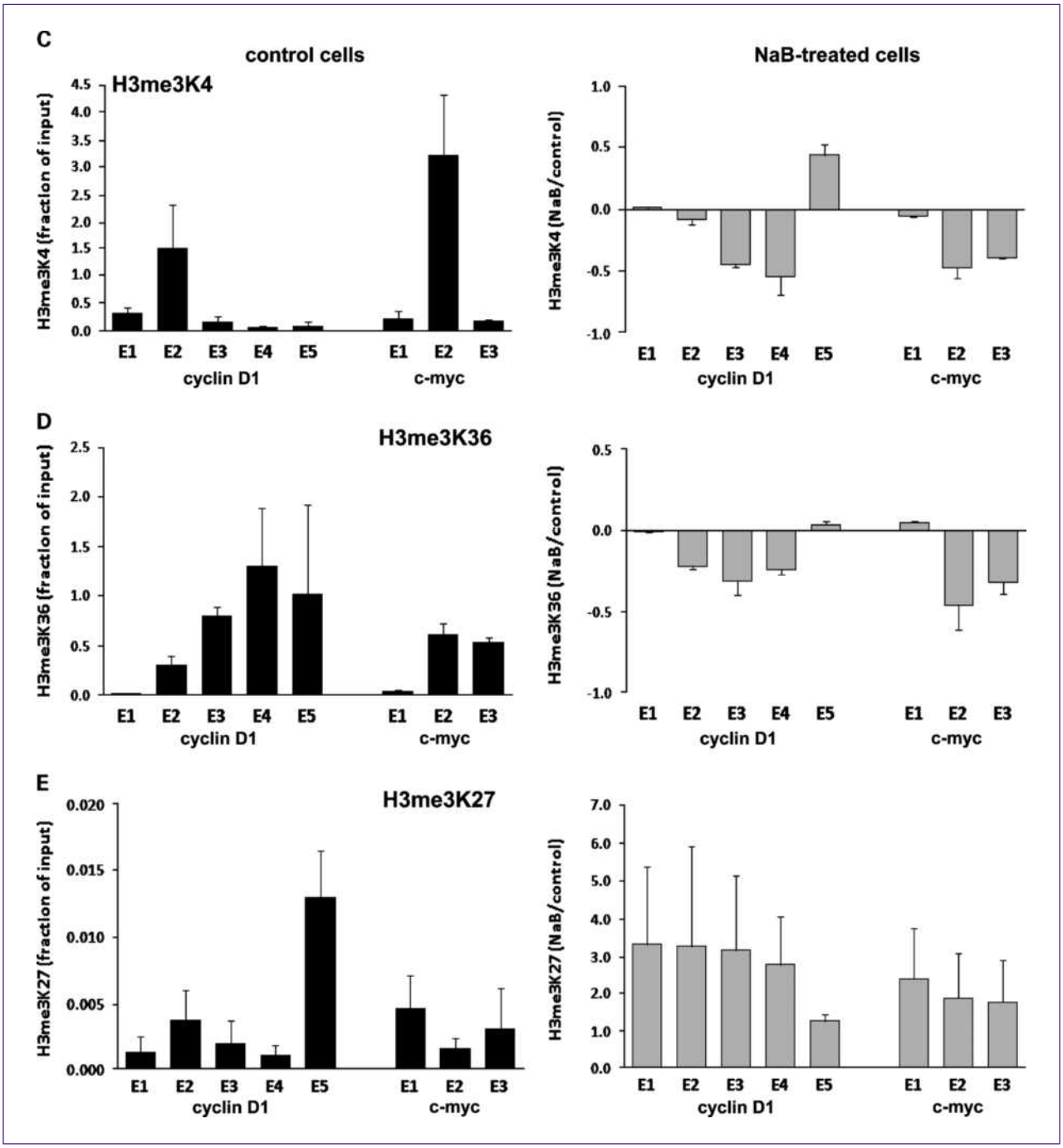

Fig. 3. ***Continued.*** C to E, H3me3K4, H3me3K36, and H3me3K27 levels. Immunoprecipitated samples were analyzed by quantitative real-time PCR and normalized by their respective input. In each case, black columns indicate basal levels in untreated cells, with data expressed as the mean ± SD of linear (C_t) values (Materials and Methods), and gray columns indicate butyrate effects, with data expressed as the ratio of NaB-treated to untreated cells. Data are from at least three independent experiments. Similar results were found at 8 h of butyrate treatment (not shown).

induces histone hypoacetylation of target genes downregulated in expression (32, 33). For both genes, a similar pattern of distribution for AcH3 as for Pol II was found in uninduced cells (Fig. 3B). However, following butyrate treatment, AcH3 levels were differentially altered along *cyclin D1*, with modest decreases associated with decreased polymerase loading at the 5′ end, whereas for *c-myc*, AcH3 remained consistently decreased, similar to the persistent decrease of Pol II (Fig. 3B). The increases in AcH3 in exons 4 and 5 of *cyclin D1* after butyrate treatment were not associated with increases in Pol II occupancy (Fig. 3A and B). This may be a technical issue because there is a human sequence *(FLJ42258)* located downstream of the *cyclin D1* gene on chromosome 11q13.2 and transcribed from the complementary strand, whose transcript is induced ~8-fold by butyrate (not shown). Hence, the elevation in AcH3 may be due to the overlap of this transcript that colocalizes with the 3′ end of *cyclin D1*.

We investigated additional histone methylation marks important in transcriptional regulation. These are trimethylated histone H3 on lysine 4 (H3me3K4), generally associated with transcription initiation; trimethylated histone H3 on lysine 36 (H3me3K36), generally associated with elongation; and trimethylated histone H3 on lysine 27 (H3me3K27), considered a mark of transcriptional silencing (32, 33). Figure 3C shows that in untreated cells, H3me3K4 was relatively higher at the 5′ end of *cyclin D1*, consistent with its role in transcription initiation, although the highest level was in exon 2, not in exon 1. Similarly, the highest level of this modification was found in exon 2 of *c-myc* (Fig. 3C). As shown in Fig. 3D, the pattern of H3me3K36 in uninduced cells was different, in each gene increasing toward the 3′ end, consistent with its association with elongation (33). Whereas there were decreases in these histone modifications along each gene following butyrate treatment (Fig. 3C and D), these were modest and generally further downstream of the marked transcriptional attenuation seen in Fig. 1A and B and, thus, may not account for this butyrate effect. Finally, the level of H3me3K27 was low along each gene (note scale of axis) and was increased by butyrate (Fig. 3E), in accordance with the role of this modification in transcriptional repression, although the data do not suggest a specific role in the attenuation of *cyclin D1* and *c-myc* by butyrate.

Similar patterns and modest histone modification in response to butyrate were seen for Caco-2 cells (Supplementary Fig. S2), with the exception of Pol II distribution, which increased at exon 1 of *c-myc*, and H3me3K4, whose levels in response to butyrate were somewhat elevated in both sequences (Supplementary Fig. S2).

Transcriptome analysis

The above studies and our prior work focused on butyrate downregulation of *cyclin D1* and *c-myc* because of the clear functional roles of these genes in colonic cell maturation and colon tumorigenesis. However, the effects of butyrate on colon carcinoma cells are highly pleiotropic, altering the expression of ~7% of sequences interrogated in our prior report (7). We therefore investigated the extent to which the regulation of transcriptional elongation contributes to downregulation of gene expression. We first used a 5′ 3′ microarray, with five probes within 100 bp of the 5′ end and 3′ end, for each of the 17,378 canonical coding sequences in GenBank (Materials and Methods). In SW837 cells untreated or treated with 5 mmol/L NaB for 2 to 12 hours, data from two independent experiments identified an overlap of 367 sequences (~2% of the sequences analyzed), the expression of which was downregulated at the 3′ end following butyrate treatment (Fig. 4A). Approximately 53% of these sequences were upregulated by butyrate at the 5′ end. For many of the remaining sequences, there were differences in the extent of downregulation at the 5′ and 3′ ends, with a large number not altered in expression at all at the 5′ end (~43%). Each of these sequences was a candidate for transcriptional attenuation downstream of the TSS.

Because butyrate can induce chromatin modification, we investigated whether the 367 sequences downregulated at the 3′ end were clustered in regions in the human genome. Figure 4B shows that there was a linear distribution of these loci as a function of the frequency of representation of genes per chromosome on the 5′ 3′ array. Therefore, there was no overall physical clustering of these sequences. A further classification by chromosomal cytoband showed that only ~12% were clustered in groups, with a maximum of four sequences per cytoband (not shown). Therefore, as for *cyclin D1* and *c-myc*, butyrate-induced transcriptional attenuation may be targeted, rather than involving broad regions affected by chromatin modification.

Recent data show that transcriptional units, previously thought to have a straight-forward organization that generates a single canonical pre-mRNA transcript, are in fact much more complex. In particular, multiple short transcripts are generated at the 5′ end as well as the 3′ end of most genes (34). Thus, there is likely to be an underlying complexity in the structure and regulation of the individual transcripts identified in Fig. 4A.

We therefore analyzed the 367 sequences downregulated at the 3′ end in response to NaB using another custom-designed microarray with probes that tile through each of these sequences, as was done for *cyclin D1* and *c-myc* (Fig. 1). Focusing on the 6- to 8-hour time period that showed the greatest changes in expression, there were 85 sequences whose 3′ end of the canonical transcript was expressed at a lower level than the 5′ end, based on the 5′ 3′ array analysis. Data from four independent experiments using the tiling array confirmed that 42 of these sequences were expressed to a significantly lower extent (>1.5-fold) toward the 3′ end than at the 5′ end and, thus, potentially paused by butyrate. Closer examination revealed that these 42 sequences fell into two general classes, which were represented equally, as shown in Table 1 and Fig. 5. Category I sequences were upregulated at the 5′ end by butyrate, but either downregulated or not significantly altered in expression further downstream, as illustrated by the *TMOD1* gene

(Fig. 5A). Twenty-eight of the 29 sequences in category I showed similar patterns of graded decrease in expression along the coding sequence, although they varied in the relative position at which expression was downregulated by butyrate. *TMEM49* sequence (NM_030938) was the exception, showing increased expression by butyrate for the first half of the sequence but an abrupt decrease at the junction of exons 10 and 11 (Supplementary Fig. S3), which could suggest induction of alternative splicing by butyrate. However, by reverse transcription-PCR and quantitative real-time PCR, we have not detected any alternatively spliced form of this gene in SW837 cells in response to butyrate (data not shown). Category II genes (Table 1) were not altered by butyrate in expression at the 5′ end, as is the case for *cyclin D1* and *c-myc* (Fig. 1), but then showed heterogeneous patterns among the sequences, which was highly reproducible across independent experiments. These patterns encompassed decreased expression, such as for *TFAP4* (Fig. 5B), or increased expression before being downregulated by butyrate, as delineated in Table 1. These patterns may result from complex transcription, characterized by multiple sites of initiation and termination as well as pausing.

The distribution of these two categories with respect to their gene ontology is shown in Table 2, with their gene IDs given in Supplementary Table SIA. The repressed targets in category I were enriched in "cytoskeleton organization" (~18%; Table 2A) and "apoptosis" (~15%), possibly contributing to the induction by butyrate of cell cycle arrest and differentiation in the cells analyzed (2, 3). In contrast, category II sequences were associated with the terms "zinc ion binding," a characteristic of many transcriptional factors involved also in transcriptional elongation (35, 36); indeed, the term "regulation of transcription" was also linked to this category (Table 2B). However, for category II, the input number of genes analyzed (Materials and Methods) was below the threshold required for assigning a *P* value. Nevertheless, the data suggest a differential pattern of transcriptional downregulation by butyrate, which may be related to different biological functions.

Table 1. Classification of transcript patterns in SW837 cells in response to butyrate

Category	Coding region			Sequences (%)
	5′ End	Middle	3′ End	
I	Up	Up	NS	47.6
	Up	Down	NS	2.4
	Up	Up/Down	Down	2.4
II	NS	Down	Down	21.4
	NS	Up	NS	16.7
	NS	Down	NS	9.5

NOTE: (A) The 42 sequences found to be potentially paused by the 5′ 3′ array and the tiling array were classified according to NaB effect throughout the canonical coding region. Up and Down indicate upregulation and downregulation, respectively (>1.5-fold change), whereas NS indicates no significant change in response to butyrate. Examples of each category are shown in Fig. 5.

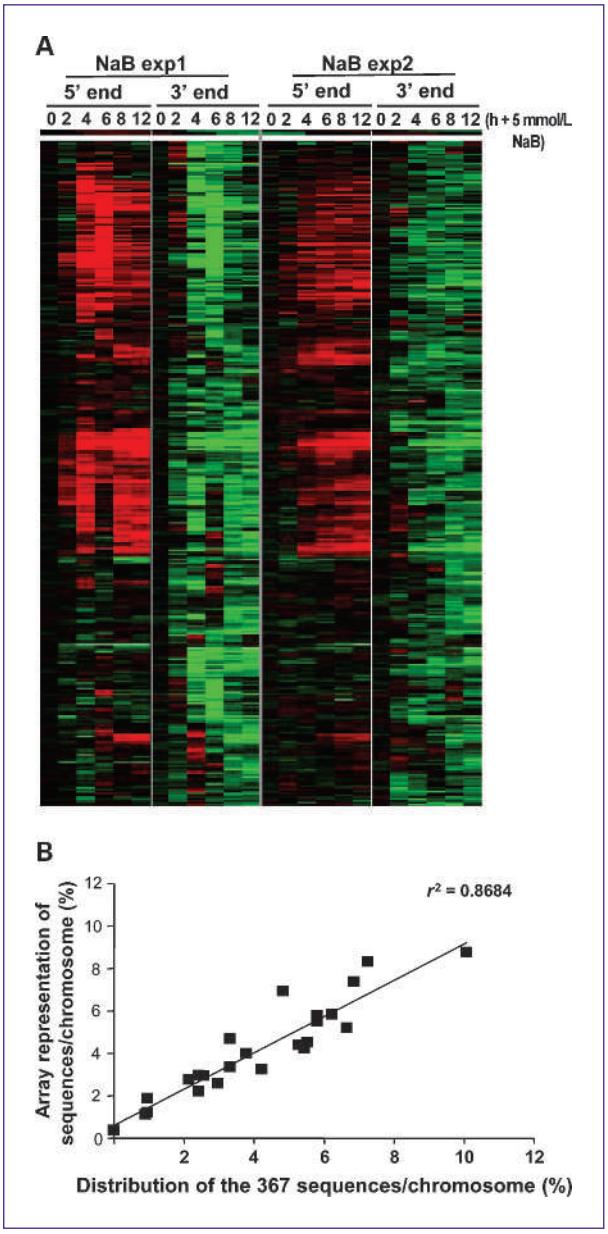

Fig. 4. Transcript expression of sequences downregulated by butyrate, assessed by the 5′ 3′ microarray. A, a total of 367 sequences were downregulated by NaB at 2 to 12 h of treatment (Materials and Methods). Data for the 5′ end are expressed as the ratio of NaB-treated to untreated cells at each time point of treatment, whereas the 3′ end data are expressed relative to the 5′ end, as the "ratio of ratios" (Materials and Methods). A heat map of two independent experiments is shown. Red and green, upregulation and downregulation in response to butyrate, respectively; black, no significant change. B, chromosome distribution of the 367 sequences downregulated by butyrate at the 3′ end relative to the sequence representation on the array.

Discussion

Butyrate, a natural dietary product and an HDAC inhibitor fundamental to normal colonic cell maturation and with potential activity in chemoprevention and chemotherapy, has extensive effects on gene expression. Butyrate alters gene expression as well as the underlying epigenetic mechanisms of transcriptional regulation (reviewed in ref. 37). We first focused on the effects on two specific genes, *cyclin D1* and c-*myc*, which are fundamental in intestinal cell maturation and tumorigenesis, and then expanded the analysis to the transcriptome level, which revealed a complexity of response to butyrate not previously appreciated.

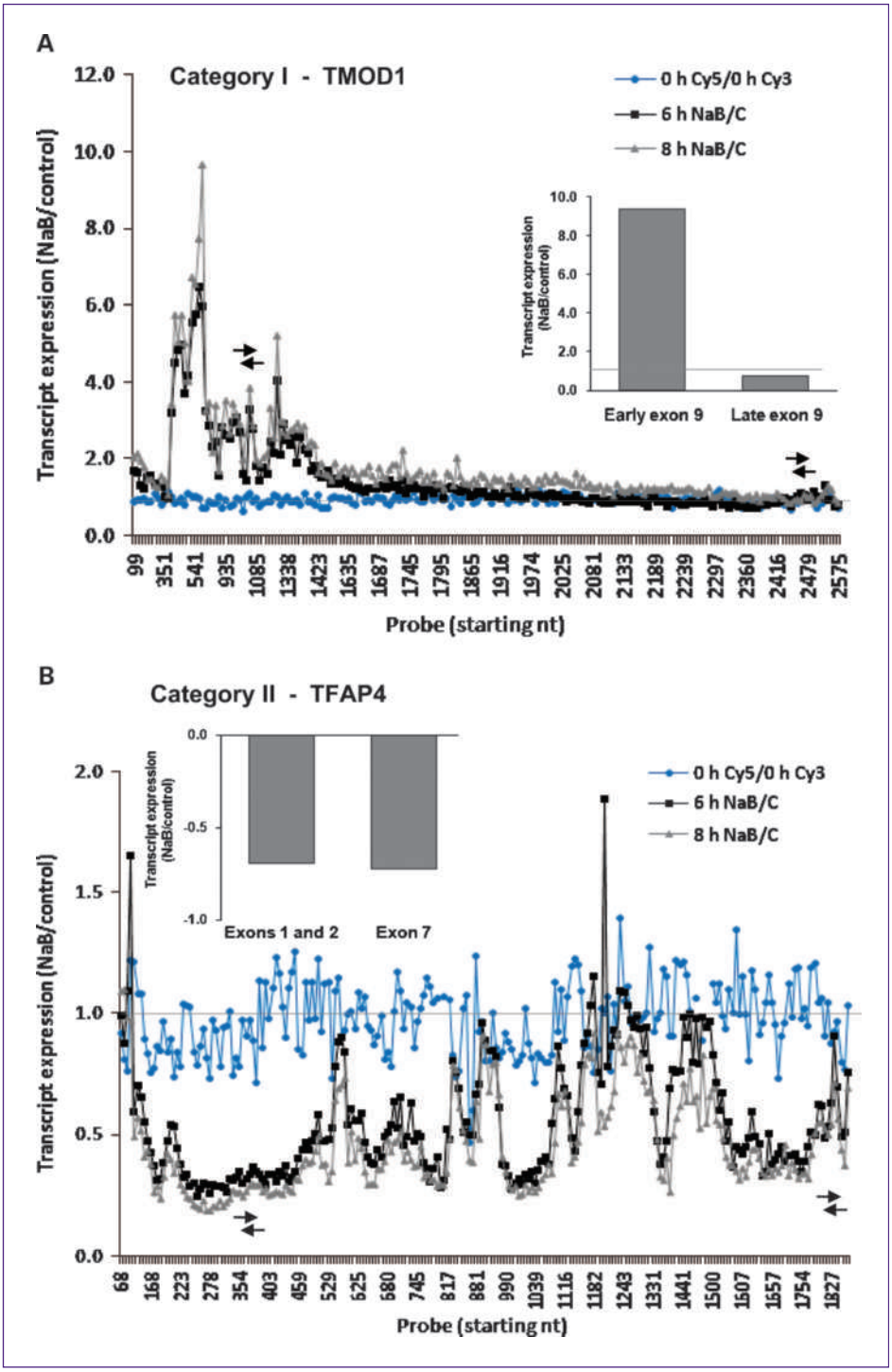

Fig. 5. Transcript expression patterns of genes downregulated by butyrate, assessed by the tiling microarray. Category I (A) and category II (B) sequences from Table 1 are exemplified by *TMOD1* and *TFAP4* genes, respectively. Data are expressed as the ratio of NaB-treated to untreated cells. Arrows indicate the regions analyzed by quantitative real-time PCR (insets, ratio of NaB-treated to untreated cells).

Transcriptional pausing was previously reported at the exon 1/intron 1 boundary of *c-myc* in hematopoietic tumor cells carrying translocations involving this gene (38, 39). Here, by using high-resolution custom-designed tiling arrays, we determined that in colon carcinoma cells, after 6 to 8 hours of butyrate treatment, there is almost a complete decrease in *c-myc* transcript expression and a marked downregulation of *cyclin D1* expression (~50%) due to a decreased steady-state level of the transcripts that begin at ~100 nucleotides downstream of the TSS (i.e., <1% and ~2% of *cyclin D1* and c-*myc* coding sequences, respectively; Fig. 1), in agreement with previous reports that transcriptional attenuation of the genes occurs close to the TSS (40). The more complete decrease in the steady-state level of *c-myc* than of *cyclin D1* transcripts may be related to the fundamental role that alterations in *c-myc* play in colon tumor development (12, 41), as well as the critical role of *c-myc* in reprogramming normal intestinal cell maturation (8). It should also be noted that deletion of only a single allele of *cyclin D1* was sufficient to decrease intestinal tumor formation in $Apc^{Min/+}$ mice, suggesting that the effects of this locus may be particularly sensitive to more modest changes in gene expression (13).

Transcriptional attenuation in the c-*myc* gene has been attributed to paused RNA Pol II and/or premature termination in the promoter-proximal region (21, 39). Whereas in Caco-2 cells, Pol II distribution increased with butyrate treatment at the very 5′ end of *c-myc*, in accord with the induction of transcriptional attenuation by butyrate in this locus, in SW837 cells butyrate inhibited Pol II occupancy toward the 5′ end of *cyclin D1* and throughout *c-myc*. In SW837 cells, butyrate-induced attenuation could be associated with a decrease in elongating polymerase complexes, as described before for other cell types (21, 42, 43).

Butyrate, a well-characterized inhibitor of HDAC activity, induced a large increase in AcH3, a mark of transcriptional activity, which we determined to occur, for example, on CDKN1A (not shown), confirming published data (44). Butyrate also induces histone hypoacetylation close to the TSS in downregulated genes (45). The butyrate-induced differences in the levels of AcH3 that we detected across the exons of *cyclin D1* and *c-myc* were generally related to Pol II occupancy. However, although they decreased toward the TSS, the AcH3 changes were modest. Similarly, basal levels of H3me3K4 were higher nearer the 5′ end of each gene, whereas H3me3K36 increased toward the 3′ end, consistent with reports that these modifications associate with transcriptional initiation and elongation, respectively, in actively transcribed genes (46, 47). However, butyrate again only modestly decreased the levels of these two modifications in both genes analyzed. On the other hand, there was a moderate increase in the levels of H3me3K27 by butyrate throughout *cyclin D1* and *c-myc*, consistent with its role in transcriptional silencing (33). Thus, although the alterations we detected in these histone marks were consistent with gene silencing by butyrate, direct correspondence with the region of attenuation was not definitive. This is consistent with the proposal that these histone modifications are not rigidly associated with the transcriptional state (26) and that the functional epigenetic landscape is more complex than previously thought (48).

Table 2. Functional classification of transcript patterns in SW837 cells in response to butyrate

A

Gene Ontology, category I sequences	Percentage	*P*
Cytoskeleton organization and biogenesis	18.5	0.001
Apoptosis	14.8	0.038
Enzyme binding	11.1	0.030
Actin binding	11.1	0.036
Caspase activation	7.4	0.036

B

Gene Ontology, category II sequences	Percentage
Zinc ion binding, zinc finger	33.3
Intracellular organelle	33.3
Regulation of transcription	22.2
Protein transport and binding	22.2
Peptidase activity	22.2
tRNA metabolic process	11.1

NOTE: The biological function and gene ontology of category I (A) and category II (B) sequences were determined by DAVID Bioinformatics database (see Materials and Methods).

Our previous data have shown that butyrate is highly pleiotropic in its effects on gene expression, with a cascade of changes that increases as a function of time following exposure, a hallmark of sequential recruitment of genes and pathways with cell maturation (7). Therefore, we pursued these widespread effects of butyrate using a whole transcriptome analysis, identifying a subset of 42 genes potentially attenuated by butyrate. Transcription of these genes, as well as of *cyclin D1* and c-*myc*, was decreased by NaB downstream of the TSS, suggesting that the initiation step of the transcriptional process was not the principal target, consistent with previous work showing transcriptional elongation as a rate-limiting step of transcription (49). Moreover, a recent report showed that in developmental systems, many genes that do not produce full-length mRNAs are nonetheless transcriptionally initiated (47).

Our transcriptome analysis revealed that whereas genes responding to butyrate fell into general categories based on the location and nature of altered expression along the coding sequence (Table 1; Fig. 5), the pattern of transcription was distinct and highly reproducible for

each gene, reflecting the high complexity of genome transcription recently elucidated (50). High-throughput parallel sequencing of transcripts should be informative in understanding this heterogeneity along these specific loci.

There are two important points regarding the complexity of transcriptional regulation by butyrate. First, butyrate is a short-chain fatty acid, consumed as a nutrient and generated by fermentation of dietary fiber, and the primary energy source for colonic epithelial cells (4). Therefore, the intestine evolved in the presence of this compound, and the complex patterns of gene expression triggered by butyrate may be key to generating the highly coordinated response that establishes and maintains the homeostasis of the colon. Second, butyrate may also exhibit antitumor properties, and the control of expression of proto-oncogenes such as c-*myc*, as well as of genes that directly promote selective advantage of tumor cells (e.g., cell growth, survival, vascularization), by transcriptional attenuation is broader than originally thought.

In conclusion, transcriptional attenuation of the *cyclin D1* and c-*myc* genes in response to butyrate begins at about 100 nucleotides downstream of the TSS. The role of chromatin remodeling and histone modification in response to butyrate is complex, may be independent of the HDAC inhibitory activity of butyrate, and may follow a gene-specific pattern. It has been proposed that control of transcriptional elongation could be a widespread mechanism of gene regulation in eukaryotes (38). Our results show that this is the case for the effects of the short-chain fatty acid butyrate and identify gene targets regulated by this mechanism.

Disclosure of Potential Conflicts of Interest

No potential conflicts of interest were disclosed.

Acknowledgments

We thank Paolo Norio, John Mariadason, Anna Velcich, and Georgia Corner for help in conducting these experiments.

Grant Support

American Institute for Cancer Research (M.C. Daroqui); National Cancer Institute grants U54CA100926, CA123473, and CA135561 (L.H. Augenlicht); and Cancer Center Support Grant P30CA13330.

The costs of publication of this article were defrayed in part by the payment of page charges. This article must therefore be hereby marked *advertisement* in accordance with 18 U.S.C. Section 1734 solely to indicate this fact.

Received 04/09/2010; revised 05/28/2010; accepted 06/10/2010; published OnlineFirst 09/14/2010.

References

1. Barnard JA, Warwick G. Butyrate rapidly induces growth inhibition and differentiation in HT-29 cells. Cell Growth Differ 1993;4:495–501.
2. Hague A, Manning AM, Hanlon KA, Huschtscha LI, Hart D, Paraskeva C. Sodium butyrate induces apoptosis in human colonic tumour cell lines in a p53-independent pathway: implications for the possible role of dietary fibre in the prevention of large-bowel cancer. Int J Cancer 1993;55:498–505.
3. Heerdt BG, Houston MA, Augenlicht LH. Potentiation by specific short-chain fatty acids of differentiation and apoptosis in human colonic carcinoma cell lines. Cancer Res 1994;54:3288–93.
4. Roediger WE. Role of anaerobic bacteria in the metabolic welfare of the colonic mucosa in man. Gut 1980;21:793–8.
5. Augenlicht LH, Anthony GM, Church TL, et al. Short-chain fatty acid metabolism, apoptosis, and Apc-initiated tumorigenesis in the mouse gastrointestinal mucosa. Cancer Res 1999;59:6005–9.
6. Heerdt BG, Augenlicht LH. Effects of fatty acids on expression of genes encoding subunits of cytochrome *c* oxidase and cytochrome *c* oxidase activity in HT29 human colonic adenocarcinoma cells. J Biol Chem 1991;266:19120–6.
7. Mariadason JM, Corner GA, Augenlicht LH. Genetic reprogramming in pathways of colonic cell maturation induced by short chain fatty acids: comparison with trichostatin A, sulindac, and curcumin and implications for chemoprevention of colon cancer. Cancer Res 2000;60:4561–72.
8. Mariadason JM, Nicholas C, L'Italien KE, et al. Gene expression profiling of intestinal epithelial cell maturation along the crypt-villus axis. Gastroenterology 2005;128:1081–8.
9. He TC, Sparks AB, Rago C, et al. Identification of c-MYC as a target of the APC pathway. Science 1998;281:1509–12.
10. Tetsu O, McCormick F. β-Catenin regulates expression of cyclin D1 in colon carcinoma cells. Nature 1999;398:422–6.
11. Sancho E, Batlle E, Clevers H. Live and let die in the intestinal epithelium. Curr Opin Cell Biol 2003;15:763–70.
12. Sansom OJ, Meniel VS, Muncan V, et al. Myc deletion rescues Apc deficiency in the small intestine. Nature 2007;446:676–9.
13. Hulit J, Wang C, Li Z, et al. Cyclin D1 genetic heterozygosity regulates colonic epithelial cell differentiation and tumor number in Apc-Min mice. Mol Cell Biol 2004;24:7598–611.
14. Heruth DP, Zirnstein GW, Bradley JF, Rothberg PG. Sodium butyrate causes an increase in the block to transcriptional elongation in the c-myc gene in SW837 rectal carcinoma cells. J Biol Chem 1993;268:20466–72.
15. Lallemand F, Courilleau D, Sabbah M, Redeuilh G, Mester J. Direct inhibition of the expression of cyclin D1 gene by sodium butyrate. Biochem Biophys Res Commun 1996;229:163–9.
16. Bender TP, Thompson CB, Kuehl WM. Differential expression of c-myb mRNA in murine B lymphomas by a block to transcription elongation. Science 1987;237:1473–6.
17. Chen Z, Harless ML, Wright DA, Kellems RE. Identification and characterization of transcriptional arrest sites in exon 1 of the human adenosine deaminase gene. Mol Cell Biol 1990;10:4555–64.
18. Mechti N, Piechaczyk M, Blanchard JM, Jeanteur P, Lebleu B. Sequence requirements for premature transcription arrest within the first intron of the mouse c-fos gene. Mol Cell Biol 1991;11:2832–41.
19. Middleton KM, Morgan GT. Premature termination of transcription can be induced on an injected α-tubulin gene in *Xenopus* oocytes. Mol Cell Biol 1990;10:727–35.
20. Tong X, Yin L, Joshi S, Rosenberg DW, Giardina C. Cyclooxygenase-2 regulation in colon cancer cells: modulation of RNA polymerase II elongation by histone deacetylase inhibitors. J Biol Chem 2005;280:15503–9.
21. Krumm A, Meulia T, Brunvand M, Groudine M. The block to transcriptional elongation within the human c-myc gene is determined in the promoter-proximal region. Genes Dev 1992;6:2201–13.
22. Raschke EE, Albert T, Eick D. Transcriptional regulation of the Igκ gene by promoter-proximal pausing of RNA polymerase II. J Immunol 1999;163:4375–82.
23. Wilson AJ, Velcich A, Arango D, et al. Novel detection and differential utilization of a c-myc transcriptional block in colon cancer chemoprevention. Cancer Res 2002;62:6006–10.
24. Zhang ZK, Davies KP, Allen J, et al. Cell cycle arrest and repression

of cyclin D1 transcription by INI1/hSNF5. Mol Cell Biol 2002;22: 5975–88.
25. Maier S, Daroqui MC, Scherer S, et al. Butyrate and vitamin D3 induce transcriptional attenuation at the cyclin D1 locus in colonic carcinoma cells. J Cell Physiol 2009;218:638–42.
26. Li B, Carey M, Workman JL. The role of chromatin during transcription. Cell 2007;128:707–19.
27. Boffa LC, Vidali G, Mann RS, Allfrey VG. Suppression of histone deacetylation *in vivo* and *in vitro* by sodium butyrate. J Biol Chem 1978; 253:3364–6.
28. Turner BM. Histone acetylation and an epigenetic code. Bioessays 2000;22:836–45.
29. Mariadason JM, Rickard KL, Barkla DH, Augenlicht LH, Gibson PR. Divergent phenotypic patterns and commitment to apoptosis of Caco-2 cells during spontaneous and butyrate-induced differentiation. J Cell Physiol 2000;183:347–54.
30. Daroqui MC, Puricelli LI, Urtreger AJ, Elizalde PV, Lanuza GM, Bal de Kier Joffe E. Involvement of TGF-β(s)/T(β)Rs system in tumor progression of murine mammary adenocarcinomas. Breast Cancer Res Treat 2003;80:287–301.
31. Sealy L, Chalkley R. The effect of sodium butyrate on histone modification. Cell 1978;14:115–21.
32. Barski A, Cuddapah S, Cui K, et al. High-resolution profiling of histone methylations in the human genome. Cell 2007;129:823–37.
33. Vakoc CR, Sachdeva MM, Wang H, Blobel GA. Profile of histone lysine methylation across transcribed mammalian chromatin. Mol Cell Biol 2006;26:9185–95.
34. Carninci P, Sandelin A, Lenhard B, et al. Genome-wide analysis of mammalian promoter architecture and evolution. Nat Genet 2006; 38:626–35.
35. Price DH. P-TEFb, a cyclin-dependent kinase controlling elongation by RNA polymerase II. Mol Cell Biol 2000;20:2629–34.
36. Tan S, Aso T, Conaway RC, Conaway JW. Roles for both the RAP30 and RAP74 subunits of transcription factor IIF in transcription initiation and elongation by RNA polymerase II. J Biol Chem 1994;269: 25684–91.
37. Kim YS, Milner JA. Dietary modulation of colon cancer risk. J Nutr 2007;137:2576–9S.
38. Bentley DL, Groudine M. Sequence requirements for premature termination of transcription in the human c-myc gene. Cell 1988; 53:245–56.
39. Keene RG, Mueller A, Landick R, London L. Transcriptional pause, arrest and termination sites for RNA polymerase II in mammalian N- and c-myc genes. Nucleic Acids Res 1999;27:3173–82.
40. Wright S, Mirels LF, Calayag MC, Bishop JM. Premature termination of transcription from the P1 promoter of the mouse c-myc gene. Proc Natl Acad Sci U S A 1991;88:11383–7.
41. Ignatenko NA, Holubec H, Besselsen DG, et al. Role of c-Myc in intestinal tumorigenesis of the ApcMin/+ mouse. Cancer Biol Ther 2006;5:1658–64.
42. Bentley DL, Groudine M. A block to elongation is largely responsible for decreased transcription of c-myc in differentiated HL60 cells. Nature 1986;321:702–6.
43. Nepveu A, Marcu KB. Intragenic pausing and anti-sense transcription within the murine c-myc locus. EMBO J 1986;5:2859–65.
44. Hinnebusch BF, Meng S, Wu JT, Archer SY, Hodin RA. The effects of short-chain fatty acids on human colon cancer cell phenotype are associated with histone hyperacetylation. J Nutr 2002; 132:1012–7.
45. Rada-Iglesias A, Enroth S, Ameur A, et al. Butyrate mediates decrease of histone acetylation centered on transcription start sites and down-regulation of associated genes. Genome Res 2007;17: 708–19.
46. Bannister AJ, Schneider R, Myers FA, Thorne AW, Crane-Robinson C, Kouzarides T. Spatial distribution of di- and tri-methyl lysine 36 of histone H3 at active genes. J Biol Chem 2005;280:17732–6.
47. Guenther MG, Levine SS, Boyer LA, Jaenisch R, Young RA. A chromatin landmark and transcription initiation at most promoters in human cells. Cell 2007;130:77–88.
48. Berger SL. The complex language of chromatin regulation during transcription. Nature 2007;447:407–12.
49. Saunders A, Core LJ, Lis JT. Breaking barriers to transcription elongation. Nat Rev Mol Cell Biol 2006;7:557–67.
50. Birney E, Stamatoyannopoulos JA, Dutta A, et al. Identification and analysis of functional elements in 1% of the human genome by the ENCODE pilot project. Nature 2007;447:799–816.